

Theoretical and Experimental Investigation of a High-Harmonic Gyro-Traveling-Wave-Tube Amplifier

D. S. Furuno,^{(1),(a)} D. B. McDermott,⁽¹⁾ C. S. Kou,⁽¹⁾ N. C. Luhmann, Jr.,⁽¹⁾ and P. Vitello⁽²⁾

⁽¹⁾*Department of Electrical Engineering, University of California, Los Angeles, California 90024*

⁽²⁾*Science Applications International Corporation, McLean, Virginia 22102*

(Received 3 August 1988)

The operation of a high-harmonic gyro-traveling-wave-tube amplifier which is based on the synchronous interaction of a rotating beam of large-orbit, axis-encircling electrons with a TE_{n1} cylindrical waveguide mode is described. Principal results include amplification of the TE_{81} mode at the eighth harmonic of the cyclotron frequency mode with a small-signal gain of 10 dB, an instantaneous interaction bandwidth of 4.3%, and a saturated power transfer of 0.5 kW.

PACS numbers: 85.10.Jz, 52.75.-d

In recent years, there has been significant interest in the potential uses of millimeter-wave devices and systems. Many applications require moderate power (1–100 kW), broadband ($\geq 5\%$) amplifiers. Conventional microwave sources do not scale well to the millimeter-wave band because of power-density limitations. The need for moderate-power millimeter-wave amplifiers has led to the examination of alternate device configurations.

The fundamental cyclotron harmonic gyro traveling wave tube (TWT)¹ has been under development for a number of years. In this device, a cloud of small-orbit, non-axis-encircling electrons interacts synchronously with a TE waveguide mode. Experimental tubes have produced 120 kW at 5 GHz with a small-signal gain of 24 dB,² 3.2 kW at 35 GHz with a small-signal gain of 52 dB,³ and 20 kW at 94 GHz with a small-signal gain of 30 dB.⁴ Unfortunately, the conventional gyro TWT requires extremely high magnetic field strengths (10–200 kG) for millimeter-wave operation. Many of the proposed applications for these amplifiers cannot tolerate the size, weight, fragility, or expense of a large magnet structure.

A configuration which allows for millimeter-wave operation using moderate magnetic field strengths is the large-orbit, high-harmonic gyro TWT. This device exhibits the same features of high power and good efficiency as the conventional gyro TWT; however, the required magnetic field is reduced in proportion to the harmonic number. Thus, the magnetic field may be obtained using a compact permanent magnet, allowing for an extremely small, lightweight, and portable system. Experimental results on high-harmonic gyrotron oscillators have included the operation of an eleventh-harmonic, 26-GHz tube with an output power of 1.5 kW.⁵ This work has recently been extended to high-harmonic gyrokystron amplifiers, with experimental results including a small-signal gain of 45 dB and an output power of 0.6 kW in a fifth-harmonic, four-cavity device operating at 11.3 GHz.⁶

In the high-harmonic gyro TWT, a cylindrical shell of large-orbit, axis-encircling electrons interacts synchro-

nously with a “whispering gallery” TE_{n1} cylindrical waveguide mode. The electrons are in resonance with the wave when

$$\omega - k_{\parallel}v_{\parallel} - n\Omega_c = 0, \quad (1)$$

where $\Omega_c = eB/\gamma m_0c$, $\gamma = [1 - \vec{v} \cdot \vec{v}/c^2]^{-1/2}$, k_{\parallel} is the axial wave vector, and v_{\parallel} is the electron’s axial velocity. In the absence of the electron beam, the dispersion relationship of the waveguide mode is

$$\omega^2 - k_{\parallel}^2c^2 - \omega_{n1c}^2 = 0, \quad (2)$$

where $\omega_{n1c} = q_{n1}c/a$ is the TE_{n1} mode’s cutoff frequency, a is the waveguide’s radius, and q_{n1} is the first zero of $J'_n(y)$. Optimum amplification occurs when the cyclotron resonance line is tangent to the waveguide’s dispersion curve or, equivalently, when the electrons’ axial velocity equals the wave’s group velocity. This condition is met if

$$n\Omega_c/\omega_{n1c} = \gamma_{\parallel}^{-1}, \quad (3)$$

where $\gamma_{\parallel} = [1 - (v_{\parallel}/c)^2]^{-1/2}$. The strongest growing frequency is then expected to satisfy

$$\omega/\omega_{n1c} = \gamma_{\parallel}. \quad (4)$$

The small-signal dispersion relation for the harmonic gyro TWT may be written as⁷

$$(\omega^2 - c^2k_{\parallel}^2 - \omega_{n1c}^2)(\omega - k_{\parallel}v_{\parallel} - n\Omega_c)^2 = \frac{4\beta_{\perp}^2\omega_{n1c}^4}{q_{n1}^2 - n^2} \left[\frac{I}{I_A} \right] \left[\frac{J'_n(q_{n1}r_{\perp}/a)}{J_n(q_{n1})} \right]^2, \quad (5)$$

where I_A represents the Alfvén current, $I_A = \beta_{\parallel}\gamma m_0c^3/e \approx 17\beta_{\parallel}\gamma$ kA. Equation (5) indicates that the coupling between the electrons and the wave is proportional to $[\beta_{\perp}J'_n(q_{n1}r_{\perp}/a)]^2$, which can be shown to approximately equal $[\beta_{\perp}J'_n(n\beta_{\perp})]^2$ by using the equation of motion. Since $J'_n(y)$ peaks for $y \approx n$, strong interaction requires very energetic electrons. Several methods for the production of high- β_{\perp} , axis-encircling electron beams are now under study at various laboratories. For the experi-

ments reported herein, gyroresonant rf acceleration was chosen.

In our gyroresonant rf accelerator, a low-energy, pencil-like electron beam is passed through a cylindrical cavity resonator which supports a large amplitude TE_{111} circularly polarized mode. The electrons gain energy from the electric field of the mode by being driven at their natural frequency and spiral outward under the influence of a longitudinal magnetic field to form a hollow, cylindrical, rotating helix whose thickness is roughly equal to the original diameter of the input beam.

This method of beam acceleration was first described by Jory and Trivelpiece.⁸ Recent investigations have shown gyroresonant rf acceleration to be a simple and efficient means of producing electron beams which are appropriate for high-harmonic gyro tubes.⁹ Experimental results have included the acceleration of 200-mA electron beams to 500 keV and peak efficiencies exceeding 50%. The fact that gyroresonant rf acceleration does not require high dc voltages is an added benefit which complements the overall aims of the high-harmonic gyro-tube concept.

A schematic diagram of the overall device configuration is shown in Fig. 1. A circularly polarized TE_{n1} mode is launched into a cylindrical waveguide with an inner radius of 2.936 cm using an azimuthal phase velocity coupler. Optimum coupling occurs when the rf wavelength in the rectangular waveguide, which is wrapped azimuthally around the interaction tube, is equal to the circumference of the cylindrical waveguide divided by n . These experiments were chosen to operate at the eighth cyclotron harmonic at a frequency of 16.2 GHz. It was evident in cold test measurements that the wave launchers were coupling to the TE_{81} mode. The transmitted power fell by more than 17 dB when a tapered section with an inner radius of 2.670 cm (which should cut off the TE_{81} mode but not the TE_{71} mode) was inserted between the two couplers. The couplers exhibited a reflection coefficient of 0.15. This would theoretically allow stable operation of the amplifier for an interaction gain of up to 16.5 dB.

In order to evaluate the device's performance, the tube was placed in a vacuum chamber within the bore of a

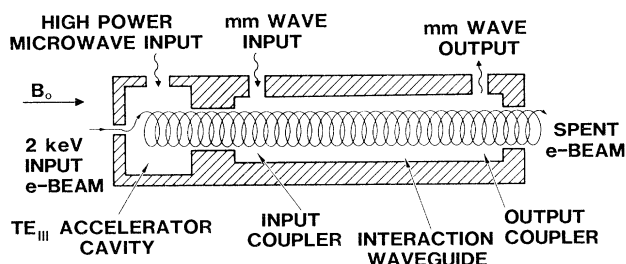


FIG. 1. Schematic diagram of the proof of principal high-harmonic gyro-TWT transmission amplifier.

laboratory solenoid. The field was tapered by 15% between the accelerator and the gyro TWT in order to increase the axial velocity of the electrons, lowering the sensitivity of the device to spatial ripple in the magnetic field profile. A peak-to-peak spatial ripple of 1.8% was measured within the interaction region, which was due to the solenoid consisting of discrete pancake magnets. Electron beam diagnostics included a current collector and current transformers for the measurement of electron beam current, a fluorescent uranium glass witness plate for the measurement of r_{\perp} , and a geometric pitch analyzer⁶ for the determination of electron pitch angle and electron pitch angle spread. Since the magnetic field strength was known, γ , β_{\perp} , β_{\parallel} , and $\Delta\beta_{\parallel}$ could be calculated.

The dependence of the observed small-signal gain on frequency is shown in Fig. 2. The bandwidth for the beam current of 150 mA is 4.3%. The beam satisfies the grazing condition [Eq. (3)] well within the 3% experimental uncertainty. However, the center frequency of 16.25 GHz corresponds to $\omega/\omega_{n1c} = (1.036 \pm 0.3)\%$, whereas from Eq. (4) the tangent intersection and thus peak gain, should occur for $\omega/\omega_{n1c} = (1.059 \pm 1)\%$. Also shown in Fig. 2 is the analytically predicted gain of the TE_{81} mode found by solving Eq. (5) and then subtracting a launching loss of 9 dB resulting from the input signal coupling to nongrowing modes. This suggests that the higher frequency waves (larger k_{\parallel}) are damped, probably from the beam's spread in axial velocity, which was measured to be $(3.5 \pm 2)\%$. This is corroborated by the final three curves in Fig. 2, which show simulation results for velocity spreads of 0%, 3%, and 5%. The numerical code was adapted from a fundamental-mode gyro-TWT code.¹⁰ The cold-beam simulation results agree quite well with the cold-beam analytical theory and the hot-beam simulation results show the expected falloff of gain at the higher frequencies.

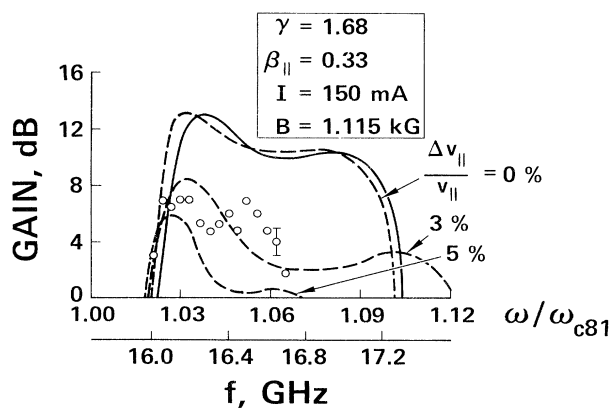


FIG. 2. Dependence of observed small-signal gain (circles) on frequency is compared to analytical theory (solid line) and simulation (dashed lines) for velocity spreads of 0%, 3%, and 5%.

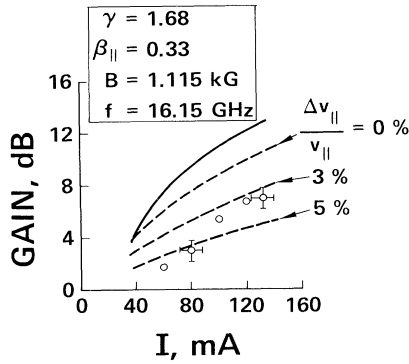


FIG. 3. Dependence of observed small-signal gain (circles) on electron beam current is compared to analytical theory (solid line) and simulation (dashed lines) for velocity spreads of 0%, 3%, and 5%.

The observed gain is plotted as a function of electron beam current in Fig. 3. Figure 3 also shows the analytical small-signal gain, found by subtracting a launching loss of 9 dB from the gain given by Eq. (5), and the results from numerical simulation of beams with velocity spreads of 0%, 3%, and 5%. The analytical theory is verified by the cold-beam simulation to within 1 dB and the simulation with a 3% spread fits the observed data to within 3 dB.

A rough estimate of the maximum possible efficiency is given by the change of γ by which the electrons advance in the wave by 180°, which can be written as

$$\pi = [n \Omega_c (\Delta\gamma/\gamma) + k_{\parallel} \Delta v_{\parallel}] \tau, \quad (6)$$

where τ is the effective duration of the interaction. It can be shown that the efficiency is then given by

$$\eta \equiv \frac{\Delta\gamma}{\gamma-1} = 2\pi\beta_{\parallel}\gamma_{\parallel} \left[\frac{\gamma}{\gamma-1} \right] \left[\frac{ck_i}{\omega_{n1c}} \right]. \quad (7)$$

For our parameters the predicted maximum efficiency is 3.5%, whereas simulation of a cold beam yields a peak efficiency of 2.2%.

The saturation characteristics of the amplifier are shown in Fig. 4. The dependence of the observed output power and implied conversion efficiency on the input power are shown together with simulation results for velocity spreads of 0%, 3%, and 5%. The maximum power transferred from the electron beam to the wave was 510 W, corresponding to an efficiency of 1.35%. The observed results agree well with the simulation results for a beam with a velocity spread of 3%, which predicts a power transfer of 470 W at an efficiency of 1.25%.

The primary limitation on the observed performance was the onset of oscillations due to reflections at the couplers. This is an engineering problem which appears to be tractable. Also, an absolute instability occurs for some values of magnetic field. In these experiments, os-

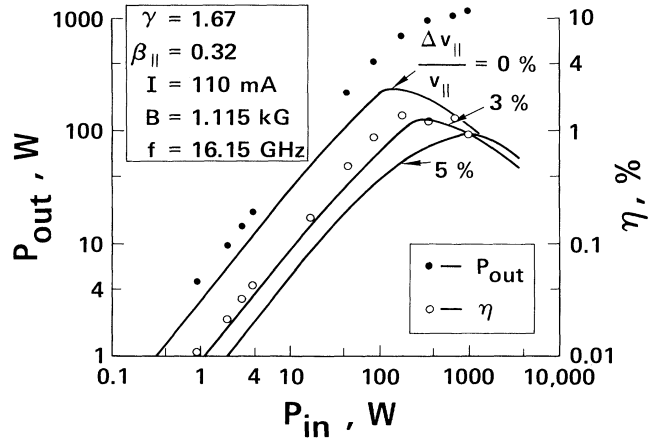


FIG. 4. Dependence of observed output power (filled circles) and efficiency (open circles) on input power is compared to simulation of efficiency for velocity spreads of 0%, 3%, and 5%.

cillations at other harmonics were not a significant problem. However, mode control will be necessary in a high-gain device.

The proof of principle experiments considered in this study were designed to demonstrate the basic operation of the high-harmonic gyro TWT. The goal was to evaluate experimental results in the context of analytic models. As a result, no attempt was made to optimize the device performance. Verification of the small-signal analytical theory and large-signal numerical simulation by the experimental results now permits the design of compact, high-gain, moderate-power millimeter-wave amplifiers based on this interaction.

The potential of a higher frequency, scaled device is of tremendous interest. A 94-GHz version, for example, operating at the eighth cyclotron harmonic using an electron beam with $\gamma=1.6$ would require only 7 kG of magnetic field. The rf accelerator for this amplifier would operate at 15 GHz. By improving the beam-to-wave coupling by increasing the electron beam current and energy, an output power of 100 kW with 10% efficiency and a gain of 5 dB/cm should be feasible. The efficiency can be enhanced by tapering the magnetic field so that electrons remain in resonance as they lose energy.² Still higher efficiencies would be obtained through the use of beam energy recovery techniques.

The authors would like to thank K. R. Chu for valuable discussions, and E. R. Kroy and H. Cao for their technical assistance. In addition, the authors would like to express their appreciation to W. H. Proud of Proud Services Corp. for his assistance in the restoration of the Hughes Aircraft Co. FLAMR radar transmitter, which was used in the saturation studies. This work was supported by U.S. Army Research Office Contract No. DAAG29-84-K-0015.

^(a)Present address: TRW, Inc., One Space Park, Redondo Beach, California 90278.

¹Y. Y. Lau, K. R. Chu, L. R. Barnett, and V. L. Granatstein, *Int. J. Infrared Millimeter Waves* **2**, 373 (1981).

²R. S. Symons, H. R. Jory, S. J. Hegji, and P. E. Ferguson, *IEEE Trans. Microwave Theory Tech.* **29**, 181 (1981).

³L. R. Barnett, J. M. Baird, Y. Y. Lau, K. R. Chu, and V. L. Granatstein, *Int. Electron. Devices Meet. Tech. Dig.* **CH1616-2**, 314 (1980).

⁴V. L. Granatstein and S. Y. Park, *Int. Electron. Devices Meet. Tech. Dig.* **CH1973-7**, 263 (1983).

⁵D. B. McDermott, D. S. Furuno, N. C. Luhmann, Jr., and P. Vitello, *Int. Electron. Devices Meet. Tech. Dig.* **CH1973-7**, 284 (1983).

⁶D. S. Furuno, D. B. McDermott, H. Cao, C. S. Kou, N. C. Luhmann, Jr., P. Vitello, and K. Ko (to be published).

⁷Y. Y. Lau, *IEEE Trans. Electron. Devices* **29**, 320 (1982).

⁸H. R. Jory and A. W. Trivelpiece, *J. Appl. Phys.* **39**, 3053 (1968).

⁹D. B. McDermott, D. S. Furuno, and N. C. Luhmann, Jr., *J. Appl. Phys.* **58**, 4501 (1985).

¹⁰A. K. Ganguly and S. Ahn, *Int. J. Electron.* **53**, 641 (1982).